Iranian Journal of Materials Forming 13 (2) (2026) 59-73

Online ISSN: 2383-0042

IJMF

Iranian Journal of Materials Forming

Journal Homepage: http://ijmf.shirazu.ac.ir

Research Article

Experimental Investigation of the Thickness Distribution in a Three-Layer Aluminum-Polyethylene Sheet During Two-Point Incremental Forming Using Central Composite Design

Mahdiye Farhadi, Behzad Soltani * and Mohammad Honarpisheh

Faculty of Mechanical Engineering, University of Kashan, Kashan, Iran

ARTICLE INFO

Article history:

Received: 1 December 2025
Reviewed: 20 December 2025
Revised: 31 January 2026
Accepted: 7 February 2026

Keywords:

Two-point incremental forming
Three-layer aluminum-polyethylene sheet
Thickness distribution

Please cite this article as:

Farhadi, M., Soltani, B., & Honarpisheh, M. (2026). Experimental investigation of the thickness distribution in a three-layer aluminum-polyethylene sheet during two-point incremental forming using central composite design. *Iranian Journal of Materials Forming*, *13*(2), 59-73. https://doi.org/10.22099/IJMF.2026.55075.1362

ABSTRACT

The two-point incremental forming (TPIF) process is an advanced and flexible method for manufacturing complex metal parts without the need for dedicated molds. In this study, the thickness distribution of three-layer aluminum–polyethylene (Al–PE–Al) sheets formed using TPIF was experimentally investigated. The sheets, measuring 180 × 180 mm and consisting of 1 mm aluminum 1050 layers and a 1 mm HDPE core, were formed into truncated pyramid geometries on a CNC machine. Using a central composite design methodology, input parameters including tool rotation speed, feed rate, and vertical step depth were varied, with thickness distribution measured as the output parameter. After forming, samples were cut using waterjet cutting to prevent thermal damage to the polymer layer. Thickness at various points along a central path was precisely measured using a vision measuring machine (VMM). Results showed that the top aluminum layer experienced greater thickness reduction than the bottom layer (23.30–39.75% vs. 12.71–32.75%) due to direct tool contact and higher local stresses. The bottom layer, protected by the polymer core, exhibited less thinning. Overall, the three-layer sheet (26.05–44.83%) showed greater thickness reduction than either aluminum layer individually, reflecting strain redistribution through the viscoelastic HDPE core and interaction between the polymer and aluminum layers. These findings emphasize non-uniform stress distribution and the importance of process parameter optimization for controlling layer-specific deformation and overall thickness uniformity.

1. Introduction

The use of multilayer sheets combining metallic and polymeric phases has grown significantly in recent years, especially in automotive and aerospace applications, due to their tunable mechanical and thermal properties, high corrosion resistance, and low weight. These characteristics make them ideal for high-performance structural components, driving increased interest in their application in precision forming and advanced manufacturing processes [1]. The heterogeneous laminar structure of multilayer

* Corresponding author
E-mail address: bsoltani@kashanu.ac.ir (B. Soltani)
https://doi.org/10.22099/ijmf.2026.55075.1362

composites leads to complex mechanical behavior and non-uniform thickness, which critically affect formability, process stability, and final part performance. However, mechanical property mismatches between layers and the risk of interfacial delamination pose significant challenges, requiring a thorough understanding of thickness evolution, interfacial adhesion, and layer integrity during forming [2]. Among advanced forming techniques, Two-point incremental forming (TPIF) has gained significant attention due to its ability to produce components with uniform thickness and enhanced control of stress fields, particularly residual stresses [3]. Nonetheless, optimizing thickness distribution and residual stress remains challenging, as numerous interacting parameters—such as applied force, temperature, tool velocity, and material properties—affect thickness in a highly nonlinear manner. Accurate characterization and prediction of these interactions require advanced statistical and computational modeling approaches [4]. Thickness reduction is an inherent feature of incremental sheet forming, caused by localized plastic deformation and material flow. In multilayer sheets, asymmetric thickness reduction between layers may lead to delamination, cracking, or mechanical degradation [5]. Among the process parameters, tool rotation speed, feed rate, and vertical step depth are the most significant factors influencing thickness reduction and surface quality. Experimental studies show that increasing vertical step depth generally increases thickness reduction and geometric deviations, while feed rate mainly regulates localized deformation. Tool rotation speed affects tool-sheet contact, thereby influencing stress distribution and material flow.

Given the complex interactions among process parameters, simultaneous statistical analysis is essential to quantify their effects on thickness reduction, surface finish, and dimensional accuracy. Such evaluations are typically performed using experimental design, mathematical modeling, and optimization techniques. Accurate identification of key parameters and rigorous assessment of their effects are crucial for ensuring desired part quality and preventing defects from asymmetric thickness reduction or uncontrolled material deformation [6, 7]. Design of Experiments (DOE) is crucial in incremental sheet forming for understanding process parameter effects and developing optimization strategies. Among DOE methods, central composite design (CCD) effectively models and optimizes multiple variables and their interactions with a limited number of experiments. Its application in multilayer sheet forming enables more precise evaluation of factors affecting thickness distribution while reducing time and cost, and has received increasing attention in recent studies [8]. Incremental sheet forming (ISF) has been extensively studied in recent years, focusing on single-point (SPIF) and two-point (TPIF) processes, multilayer and composite sheets, and process optimization strategies.

Single-point incremental forming (SPIF): SPIF research has examined the effects of process parameters on forming force, thickness distribution, dimensional accuracy, and springback. Ghasemi and Soltani [9] investigated forming force and thickness distribution in SPIF. Honarpisheh et al. [10] studied springback in explosively welded Cu/St/Cu three-layer sheets. Rezaei and Honarpisheh [11] evaluated forming limit diagrams (FLDs) in CP-Ti/St12 bimetal sheets. Deilami Azodi et al. [12, 13] explored thickness variation and optimized AA3105-St12 bimetal sheets using SPIF in combination with artificial neural networks (ANN) and multi-objective genetic algorithms (MOGA). Esmaeilian et al. [14] investigated fracture depth in metal–polymer–metal three-layer sheets. Tayebi and Hashemi [15] assessed SPIF limitations for Al-Mg bimetal sheets, and Tayebi et al. [16] examined FLDs in Al/Cu bimetal sheets.

Two-point incremental forming (TPIF): TPIF studies have emphasized thickness uniformity, residual stress management, and geometric accuracy. Shawkiang et al. [17] analyzed geometric errors in TPIF of Al-Cu-Mg alloys. Lu et al. [18] studied thickness uniformity in stepped components. Visagan and Ganesh [19] optimized TPIF parameters using grey relational analysis (GRA) and TOPSIS, while Singal et al. [20] focused on residual stress optimization. Manoj et al. [21] compared SPIF and TPIF combined with ultrasonic-assisted techniques to enhance formability.

Multilayer and composite sheets: Forming multilayer and composite sheets poses additional challenges due to their complex mechanical behavior. Harhash and Palkowski [22] studied steel–polymer–steel composites. Thomas et al. [23] investigated metal-based composites for aerospace and automotive applications. Zhao and Hangan [24, 25] introduced flexible multi-point incremental forming (F-MPIF-MLS) and hybrid stretch forming combined with double-layer TPIF. Seçgin et al. [26] proposed a multi-stage incremental forming approach. Fabian et al. [27] addressed residual stresses using flexible stress superposition.

Process optimization and modeling: Several studies have integrated experimental investigations with modeling and optimization to improve process understanding. Deilami Azodi et al. [13] combined SPIF with ANN and MOGA for multilayer sheets. Visagan and Ganesh [19] applied GRA and TOPSIS for TPIF parameter optimization. These approaches demonstrate the importance of systematic evaluation of process parameters to achieve optimal thickness distribution and high part quality.

Despite these advances, comprehensive investigations on the thickness distribution of aluminum–polyethylene multilayer sheets in TPIF using a central composite design (CCD) approach remain limited. Moreover, experimental data and response surface modeling for process optimization are insufficiently addressed in recent literature. The present study addresses this gap by conducting a systematic experimental investigation of thickness distribution in aluminum–polyethylene three-layer sheets during TPIF using a CCD methodology. The main process parameters are varied, and the thickness distribution of a truncated pyramid with a square cross-section is measured. The data are analyzed through statistical analysis and response surface modeling, providing insights for optimizing forming conditions and enhancing part quality.

2. Materials and Method

2.1. Materials and sample preparation

In this study, three-layer sheets were fabricated via a hot-pressing method. The structure comprised two aluminum layers, each 1 mm thick, positioned on the top and bottom, with a polyethylene core derived from maleic powder (Fig. 1). The aluminum sheets and polymer powder were arranged in an aluminum–powder–aluminum configuration and subjected to a pressure of 30 tons at 150 °C, allowing the polymer powder to melt and establish a strong mechanical bond with the aluminum layers. This process produced uniform three-layer sheets, approximately 3 mm thick, without using adhesives or lateral mechanical fasteners.

2.2. Experimental equipment and sample geometry

In the two-point incremental forming (TPIF) process, a die is positioned beneath the sheet, in addition to the forming tool and sheet holder, allowing deformation to occur at two contact points: one between the tool and the sheet surface, and the other between the sheet and the die at its bottom surface.

In the present study, forming experiments were conducted at room temperature using a Siemens CNC milling machine equipped with a 10 mm diameter spherical Mo40 steel tool, while a steel die was positioned beneath the sheet (Fig. 2).

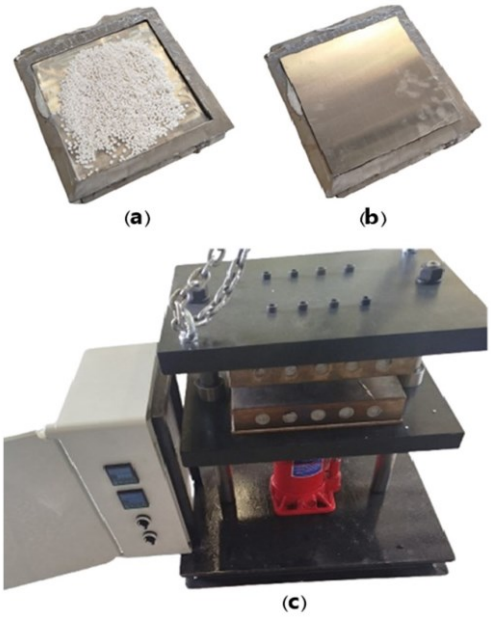

Fig. 1. Steps for preparing three-layer sheets using the hot pressing method: (a) placing maleic powder on the lower aluminum sheet, (b) placing the upper aluminum sheet on the powder layer, (c) placing the sheets inside the hot press machine.

Fig. 2. General view of the two-point incremental forming (TPIF) process.

Due to the tool's moderate friction coefficient and the potential risk of thermal damage at the tool tip, sufficient lubrication was applied to the sheet surface throughout the forming process. The specimens were formed into truncated square pyramids with predefined dimensions (Fig. 3), enabling precise evaluation of thickness distribution and complex deformation behavior.

2.3. Process parameters and experimental design

For conducting these experiments, the design of experiments (DOE) approach was employed. Tool speed, feed rate, and vertical step depth were considered as the primary factors influencing the process, while layer thickness distribution served as the response variable. The parameter ranges were established based on preliminary experiments, insights from previous studies, and the operational constraints of the equipment. To thoroughly assess linear, quadratic, and interaction effects, a central composite design (CCD) was utilized, incorporating factorial, axial, and center points to enhance the model's accuracy. The CCD experimental design is presented in Table 1.

2.4. Sample cutting and thickness measurement

After forming, the samples were cut in half using a waterjet cutting method for thickness measurement (Fig. 4).

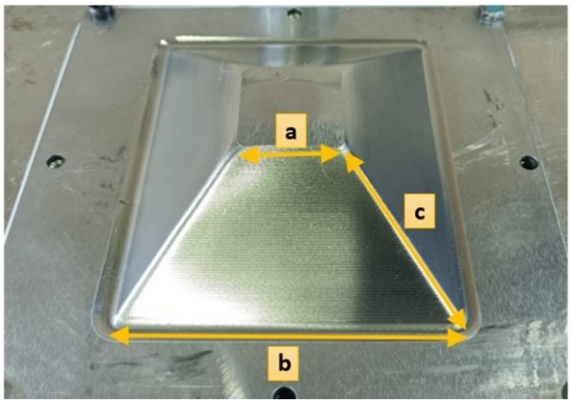

Fig. 3. The geometry of the specimen produced through the two-point incremental forming (TPIF) process: a = 20 mm, b = 100 mm, and c = 55 mm.

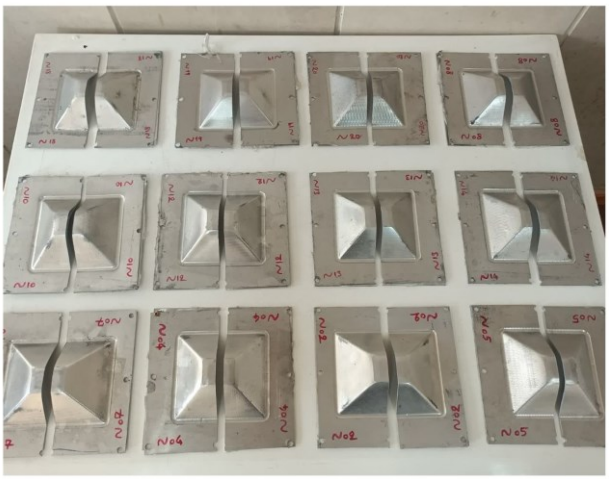

Fig. 4. Samples subjected to waterjet cutting.

Table 1. Central composite design (CCD) experimental layout generated using Minitab software

Number	Feed rate (mm/min)	Rotation speed (rpm)	Vertical step depth (mm)
01	1500	1500	0.75
02	1000	2000	0.5
03	1500	1500	0.75
04	1500	1500	0.33
05	2000	1000	0.5
06	1500	1500	0.75
07	2000	2000	1
08	1000	1000	0.5
09	1000	1000	1
10	2000	1000	1
11	1500	1500	0.75
12	1000	2000	1
13	659	1500	0.75
14	2340	1500	0.75
15	1500	1500	0.75
16	1500	1500	0.75
17	2000	2000	0.5
18	1500	2340	0.75
19	1500	1500	1.17
20	1500	659	0.75

Waterjet cutting was selected because it avoids inducing thermal or mechanical alterations in the samples' structure and thickness. Following the cutting process, the thickness of the aluminum and polyethylene layers was determined using a Vision Measuring Machine (VMM) (Fig. 5). Due to the symmetry of the sample geometry, thickness distribution measurements were conducted along the path illustrated in Fig. 6.

Moreover, the uniformity of the thickness of the middle layer (PE) along a specific path in the x and y directions **(**after the hot pressing process) was checked with a non-contact measuring device (Vision Measuring Machine) with a repeatability of 2 µm and a resolution of 1 µm (Fig. 7). The results showed that it had a high degree of uniformity with an approximate error of less than 0.1%.

2.5. Tensile test

In the present study, to extract the mechanical properties of the sheets, uniaxial tensile tests were performed for aluminum and polyethylene specimens (Fig. 8).

The obtained stress-strain curves for aluminum and polyethylene are shown in Fig. 9.

3. Results and Discussion

3.1. Thickness distribution analysis

In this section, the thickness distribution of the top and bottom aluminum layers, as well as the overall thickness of the three-layer sheets, is analyzed. As shown in Figs. 10, 11, and 12, the thickness profiles obtained along the predefined measurement path are presented for all five specimens. These profiles allow for a direct comparison of the deformation behavior under varying process parameters, including feed rate (f), spindle speed (v), and vertical step depth (p). Overall, the results reveal a consistent trend of thickness reduction with increasing forming depth across all specimens.

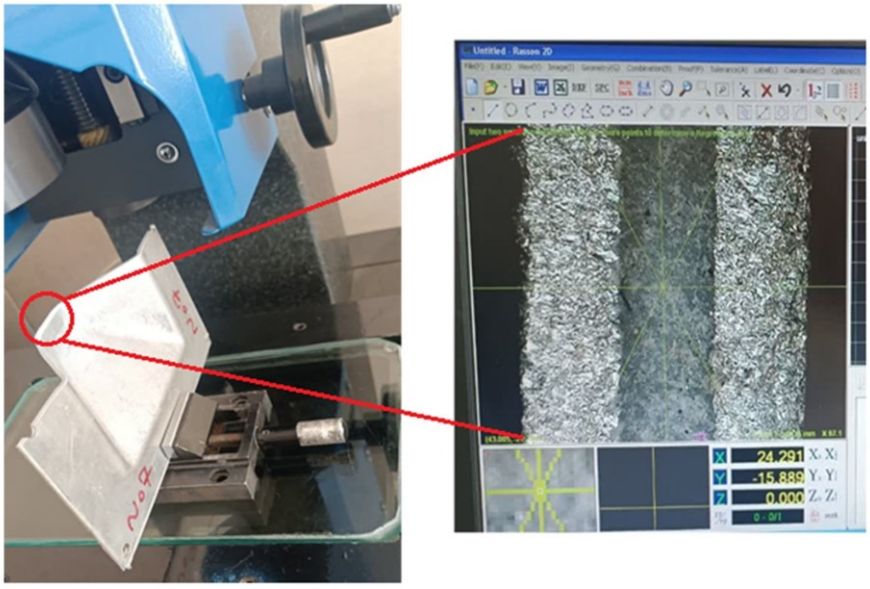

Fig. 5. Thickness measurement of the layers in the formed samples using a Vision Measuring Machine (VMM).

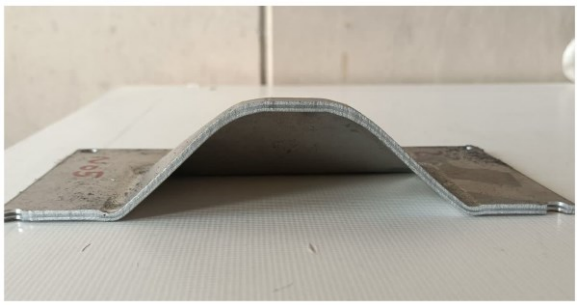

Fig. 6. Measurement path for thickness distribution in the samples.

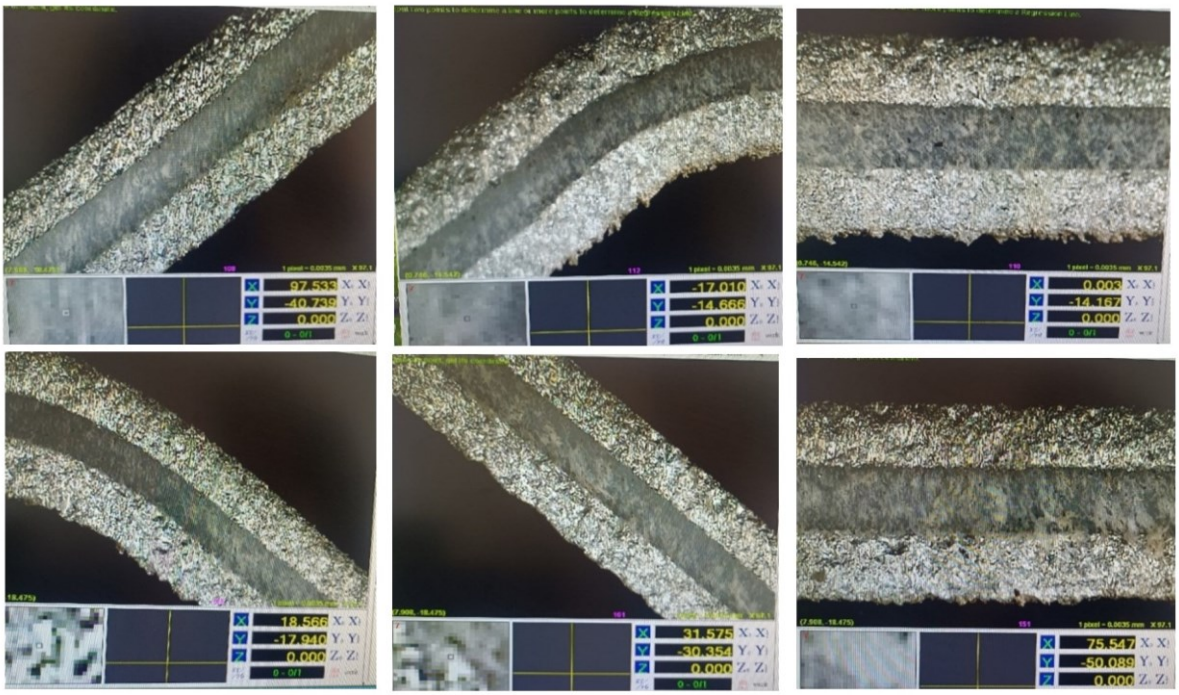

Fig. 7. The uniformity of the 3 layers' thickness along a specific path in the x and y directions (is indicated in yellow at the bottom of the image).

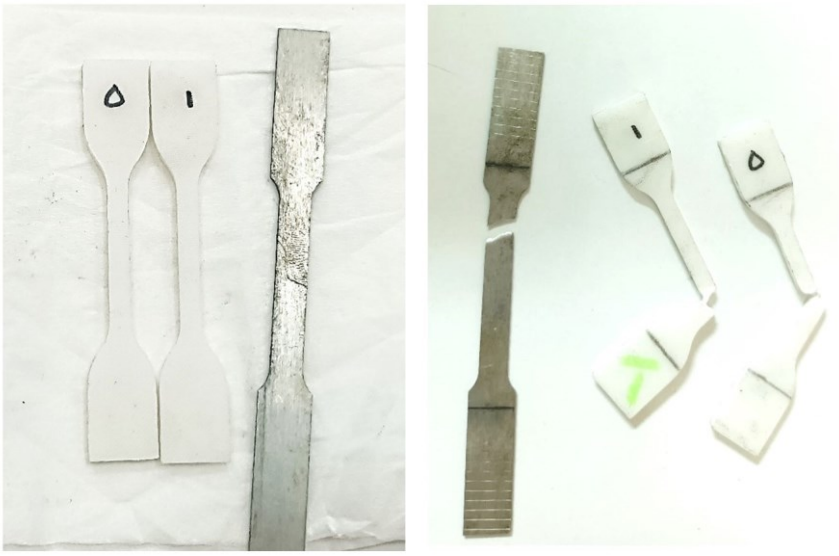

Fig. 8. Uniaxial tensile test specimens of aluminum and polyethylene sheets, respectively, according to standard ASTM E8 and ASTM D638.

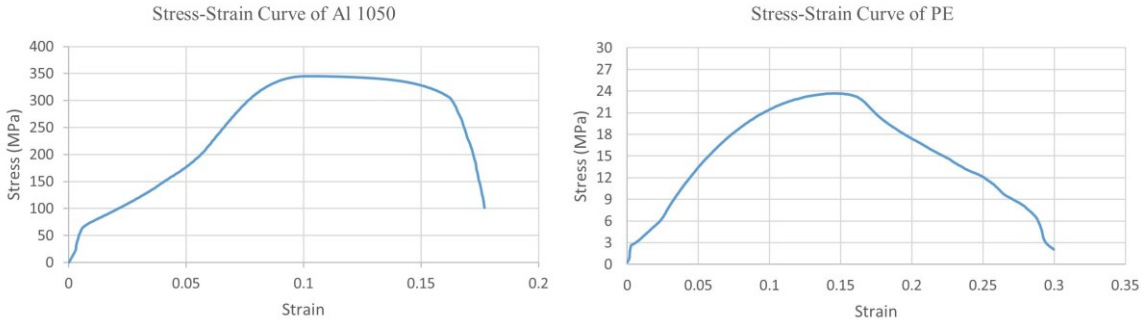

Fig. 9. Stress-strain curves from tensile test for single-layer samples.

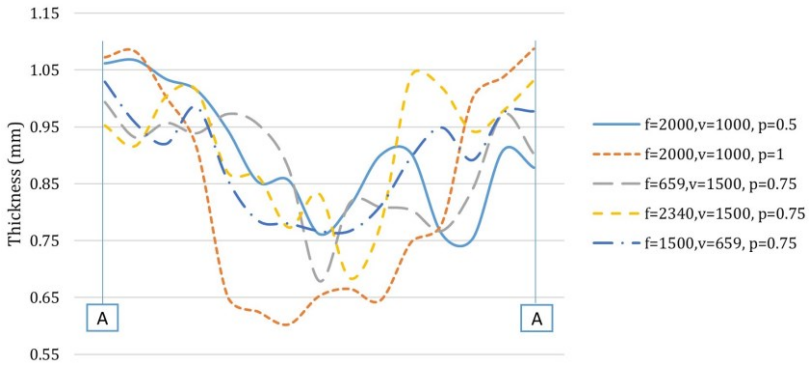

Fig. 10. Thickness distribution chart of the top aluminum sheets with different parameters according to Table 1.

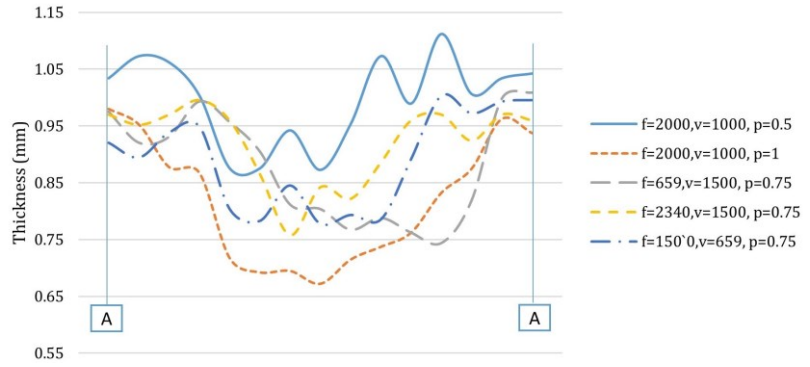

Fig. 11. Thickness distribution chart of the bottom aluminum sheets with different parameters according to Table 1.

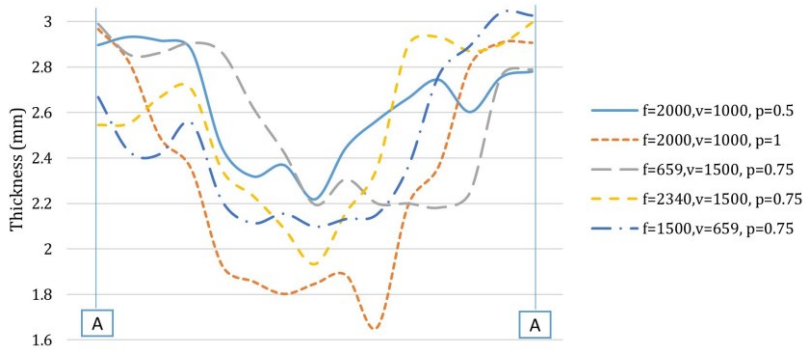

Fig. 12. Thickness distribution chart of the 3-layered sheets with different parameters according to Table 1.

This behavior is characteristic of the two-point incremental forming (TPIF) process, in which dominant in-plane tensile stresses induce localized thinning along the tool path. Regions closer to the tool trajectory experience higher strains and, consequently, exhibit more pronounced thickness reduction, whereas regions farther from the trajectory undergo minimal deformation. A comparison of the individual layers indicates that the upper aluminum layer, which is in direct contact with the forming tool, undergoes greater thinning than the lower layer. The direct interaction with the tool induces higher localized strains and concentrated stresses in the upper layer. In contrast, the lower aluminum layer, primarily influenced by deformation transmitted through the polyethylene core, experiences more uniformly distributed stresses and, consequently, a lower degree of thickness reduction. The total laminate thickness further confirms that the majority of deformation occurs within the metallic layers, while the polyethylene core serves as a stress-absorbing medium that mitigates localized strain concentrations.

The influence of process parameters is also evident in the obtained thickness profiles. An increase in feed rate leads to more pronounced thinning in both aluminum

layers, due to reduced material flow time and elevated localized strains. In contrast, an increase in spindle speed results in less thinning, which can be attributed to a localized temperature rise, enhanced material flowability, and more uniform strain distribution. Furthermore, increasing the vertical step-down amplifies thickness reduction and introduces greater non-uniformity in the thickness profile, as larger incremental depths generate higher instantaneous forming loads and more concentrated strain fields.

3.2. Thickness reduction percentage

The thickness reduction percentages of the individual aluminum layers and the three-layer sheets were measured, and the corresponding values are summarized in Table 2.

As shown, the top aluminum layer undergoes a substantially higher percentage of thickness reduction compared to the bottom layer. This pronounced thinning in the upper layer is primarily attributed to its direct interaction with the forming tool. During each incremental forming step, the upper layer experiences the highest local contact pressures and is consequently subjected to larger in-plane tensile stresses and concentrated plastic strains. This results in a more intense deformation response relative to the lower aluminum layer, which is partially shielded by the intermediate polyethylene core and thus experiences a more attenuated stress field. Furthermore, the total thickness reduction observed in the three-layered sheet is notably greater than that in the single-layer aluminum sheet. The presence of the polyethylene core between the metallic layers plays a crucial role in modifying the deformation behavior of the system. The polymer layer facilitates additional deformation by redistributing the applied stresses and enabling more uniform strain accommodation throughout the laminate. Its comparatively lower stiffness allows localized material flow within the structure, reducing constraints on the metallic layers and promoting enhanced plastic deformation.

In other words, this behavior arises from the complex mechanical interaction between layers and the distinct material properties of each constituent. The aluminum layers, exhibiting elasto-plastic behavior, resist deformation, whereas the middle polyethylene layer behaves as a soft viscoelastic material capable of large deformations under both short-term and long-term loading. During double-point forming, the viscoelastic core flows and undergoes significant thickness reduction. This core deformation induces additional thinning in the aluminum layers to maintain the geometric and structural equilibrium of the laminate. In essence, the viscoelastic response of the middle layer redistributes stresses among the layers, increasing the overall laminate thinning relative to that of the individual layers, even if each aluminum layer is limited by its own plastic capacity. This observation is consistent with multilayer mechanical analyses and theoretical modeling reported in the literature, which indicate that a soft viscoelastic core promotes localized deformation and amplifies overall thinning. Therefore, the enhanced overall laminate thinning can be directly attributed to the viscoelastic behavior of the middle layer and represents a fundamental mechanism governing the forming behavior of multilayer laminates

Table 2. Thickness reduction percentage of the aluminum layers and three-layered sheets

Samples	Top Al sheet reduction (%)	Bottom Al sheet reduction (%)	Three-layer sheet reduction (%)
01	29.80	31.10	26.77
02	20.35	21.97	24.04
03	28.11	32.4	27.37
04	31.84	36.16	26.16
05	24.66	12.71	26.05
06	30.14	31.05	28.44
07	29.54	24.86	23.56
08	28.88	25.24	30.19
09	35.52	31.10	31.11
10	39.75	32.75	44.83
11	28.92	31.74	27.52
12	26.58	28.45	34.48
13	32.14	25.64	27.29
14	31.65	24.22	35.57
15	28.66	29.84	25.43
16	29.31	32.72	27.56
17	28.62	23.12	22.55
18	25.48	24.13	24.31
19	25.47	24.65	26.85
20	23.30	22.26	32.31

3.3. Effect of process parameters

Analysis of variance (ANOVA) indicates that the vertical step depth exerts the greatest influence on the overall thickness reduction, particularly in the upper aluminum layer, as it directly governs the amount of deformation at each incremental step. Tool rotation speed and feed rate have comparatively smaller effects, primarily affecting friction conditions and strain rates. Response surface plots generated from the CCD data (Figs. 13-16) reveal complex interactions among the process parameters. Optimized parameter combinations that minimize thickness reduction while preserving dimensional accuracy were identified. These models facilitate the prediction of forming process outcomes and the selection of optimal parameters.

3.4. Finite element modeling

Finite element simulations of the incremental sheet forming process under dynamic loading conditions (for sample N01) were conducted using the ABAQUS/Explicit solver.

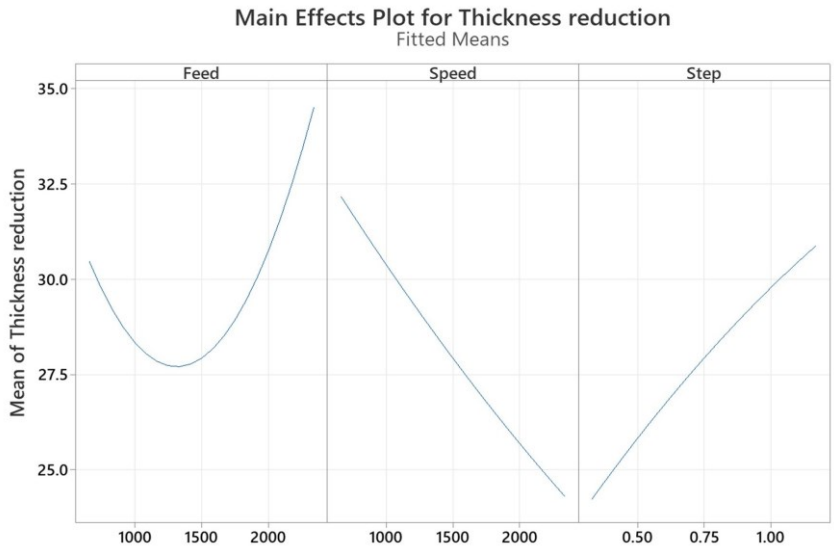

Fig. 13. Main effects plot for thickness reduction.

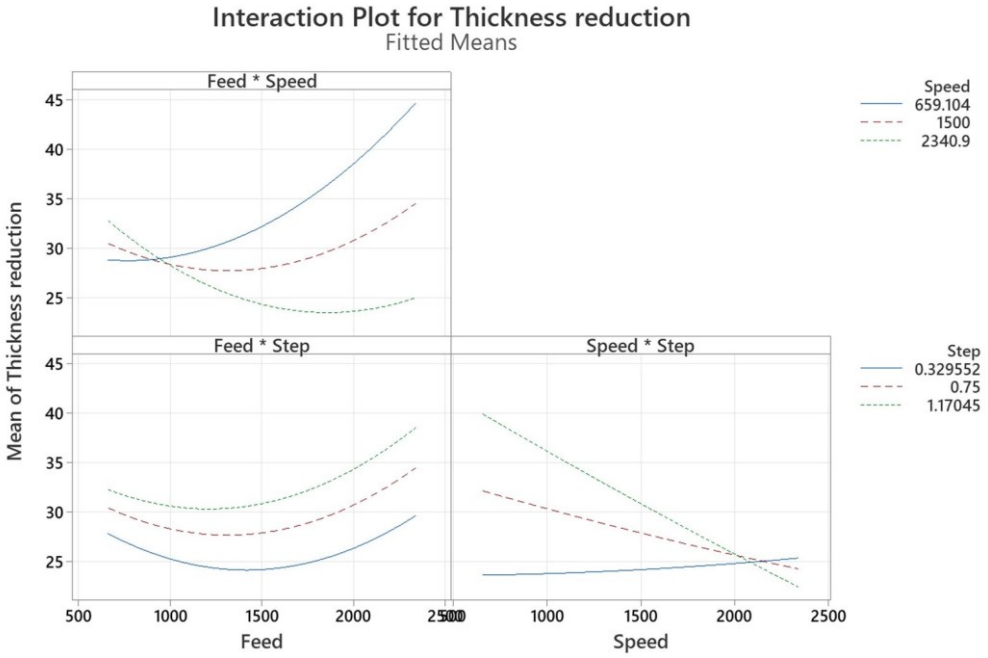

Fig. 14. Interaction plot for thickness reduction.

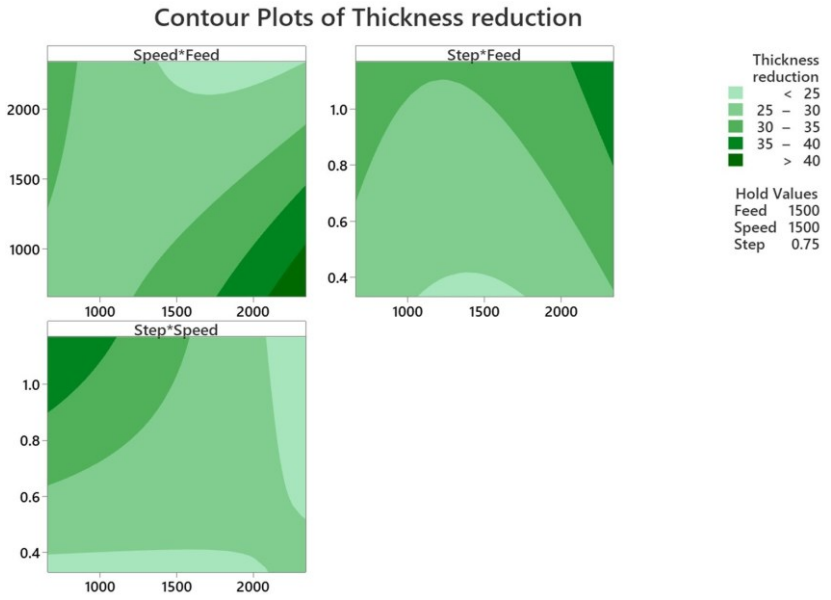

Fig. 15. Contour plots of thickness reduction.

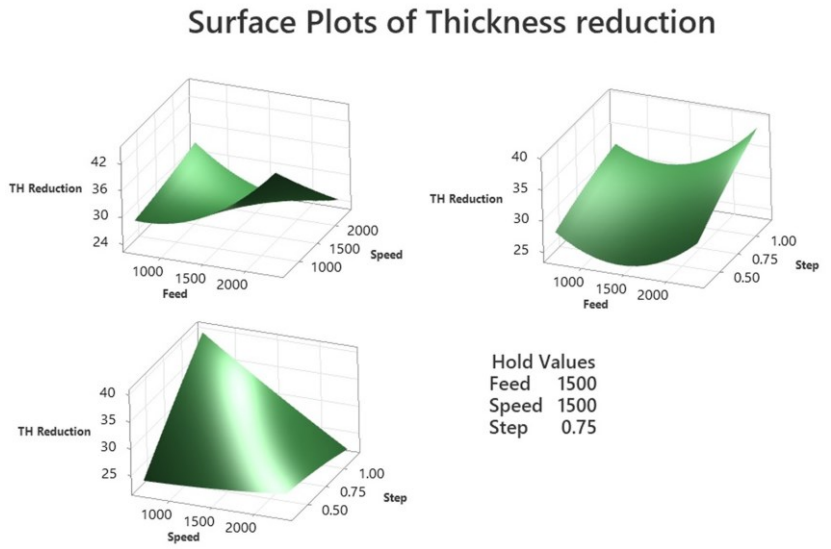

Fig. 16. Surface plots of thickness reduction

To achieve a balance between computational efficiency and numerical accuracy, the sheets were discretized using four-node shell elements (S4R) with reduced integration and hourglass control. An initial element size of 5 mm was adopted, and following a mesh sensitivity analysis, a refined element size of 2 mm was selected for the final simulations. In the numerical model, the holder plate was located above the sheet assembly, while the pyramid-shaped die was positioned beneath the sheets. The forming tool was placed at an appropriate distance above the top sheet prior to the forming operation. Surface-to-surface contact interactions were defined between the forming tool and the top sheet, the die and the bottom sheet, as well as between the holder plate and the top sheet. All contact interfaces were modeled using a penalty-based friction formulation with a friction coefficient of 0.15. The overall finite element model employed in the simulations is shown in Fig. 17.

The material behavior of the aluminum and polyethylene layers was defined using the corresponding stress–strain curves presented in Fig. 9. The influence of strain rate on the yield stress was neglected in the present simulations. To investigate thickness variation along the formed geometry, a reference path was defined along the

inclined wall of the truncated square pyramid, extending from the larger base toward the smaller base (Fig. 18) and the thickness distribution along this path was extracted and analyzed. In addition, the thickness distribution on the deformed model is shown in Fig. 19. Figs. 20 and 21 illustrate the thickness profiles of the bilayer and three-layer sheets formed by the two-point incremental forming (TPIF) process.

The results demonstrate a gradual decrease in thickness with increasing forming depth, with the most severe thinning occurring on the wall of the pyramid where the wall angle is highest.

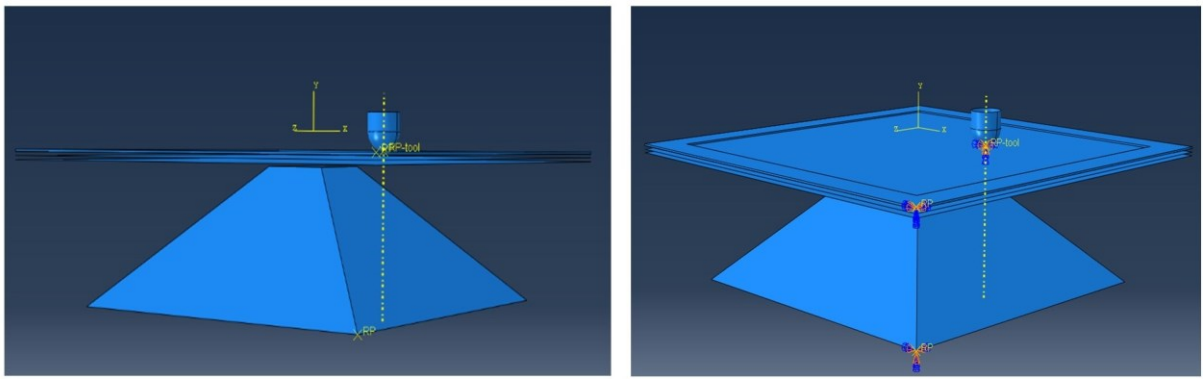

Fig. 17. Stress–strain curves: (a) four-pass and (b) eight-pass processed samples.

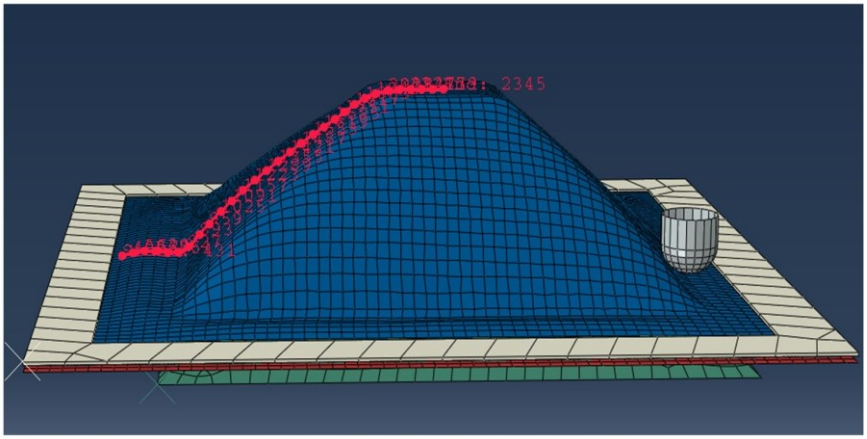

Fig. 18. Measurement path for thickness distribution in Abaqus software.

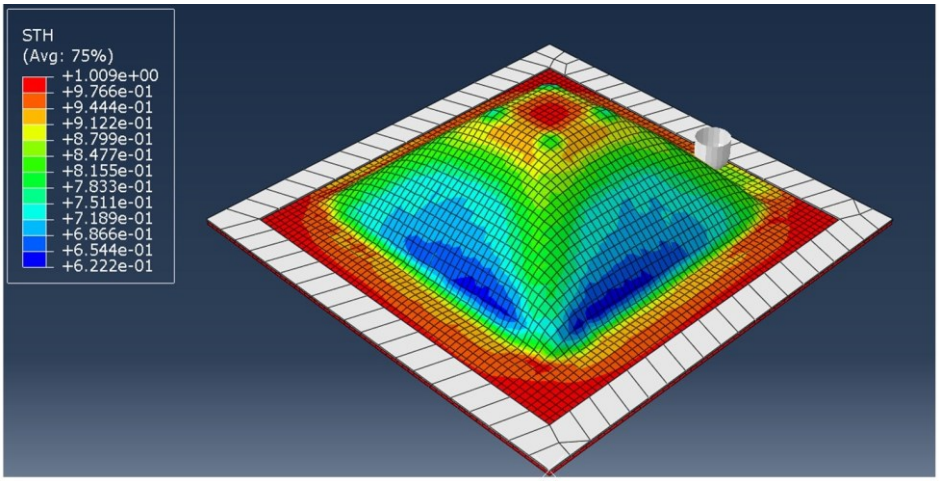

Fig. 19. The thickness distribution on the deformed model in Abaqus software.

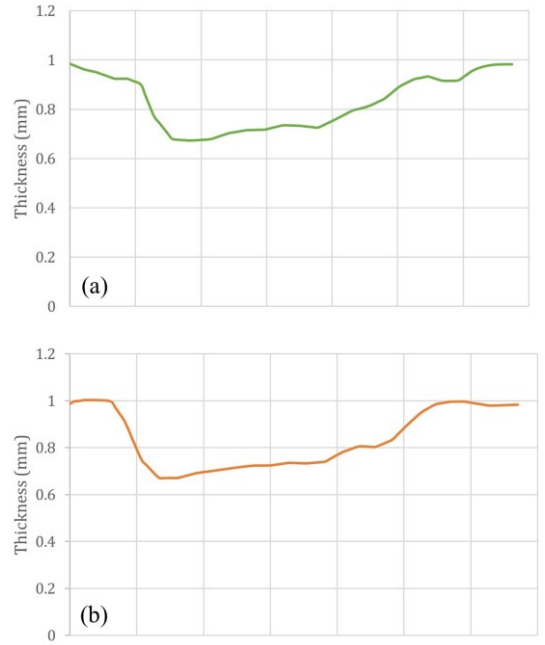

Fig. 20. The thickness distribution diagram of the deformed bilayer sheet: (a) upper and (b) bottom sheet along the specified path in Fig. 18 resulting from simulation.

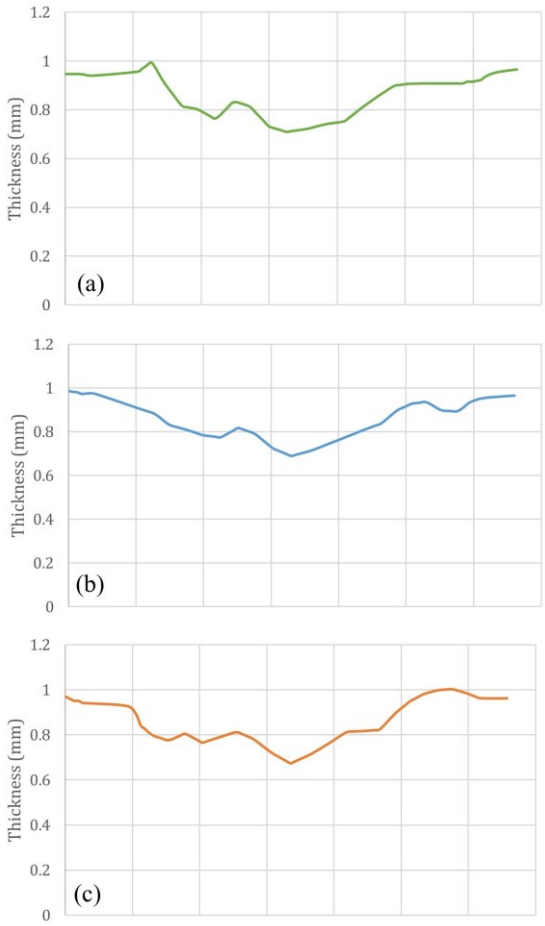

Fig. 21. The thickness distribution diagram of the deformed three-layered sheet: (a) upper, (b) middle, and (c) bottom layers along the specified path in Fig. 18 resulting from simulation.

A comparison between the numerical thickness distribution and the predictions of the sine law was also performed. While the general trends were in reasonable agreement, noticeable deviations were observed near the lower region of the formed part. These discrepancies are mainly attributed to the complex tool–sheet contact conditions and the heterogeneous deformation behavior arising from the laminated sheet configuration. Figs. 20 and 21 show the thickness distribution of individual layers after two-point growth forming of a truncated square pyramid for laminates with and without a polyethylene interlayer. In both cases, the maximum thinning occurs along the sloping sidewalls, while the upper region shows relatively limited thickness reduction. For the laminate containing the polyethylene interlayer, the thinning is more uniformly distributed along the sidewalls, with a smooth thickness gradient and no significant local thinning. Both aluminum layers show similar thinning patterns, indicating a coordinated deformation behavior. In contrast, the laminate without the interlayer shows significant thickness non-uniformity along the sidewalls, characterized by local thinning and a steep thickness gradient. The limited interfacial shear deformation in this configuration exacerbates strain localization under loading. In general, the presence of the polyethylene interlayer improves thickness uniformity along the pyramid walls by facilitating strain redistribution and reducing local thinning during forming.

Finally, a comparison of experimental and simulated thickness distributions for the upper and bottom aluminum sheets of sample N01 is shown in Fig. 22. As can be seen, there is acceptable agreement between the results from finite element simulation and experimental tests.

4. Conclusions

In this study, the thickness distribution of three-layer aluminum–polyethylene (Al–PE–Al) sheets formed via the two-point incremental forming (TPIF) method was experimentally investigated. Hot pressing proved effective in producing uniform, integrated sheets, while waterjet cutting enabled damage-free sectioning and

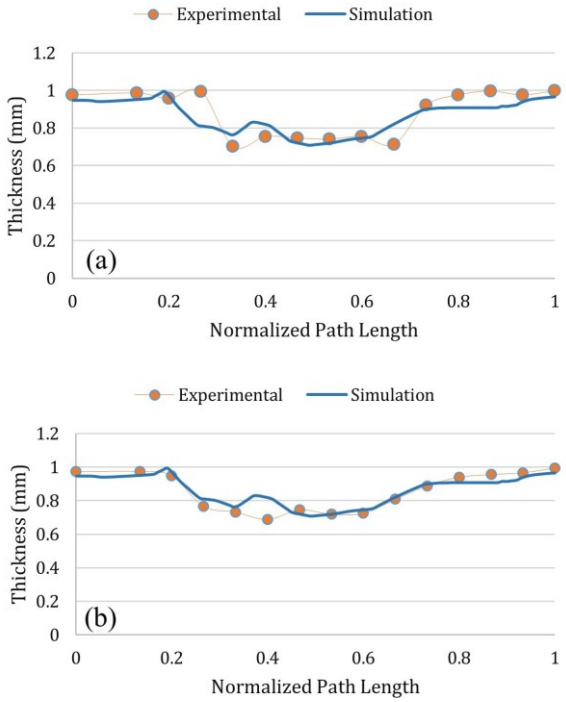

Fig. 22. Comparison of experimental and simulated thickness distributions for (a) the upper and (b) the bottom aluminum sheets of sample N01.

precise thickness measurements. The TPIF behavior of Al–PE–Al sheets was examined, focusing on the effects of process parameters on thickness distribution, deformation mechanisms, and overall formability. The experimental results demonstrated that the upper aluminum layer undergoes the most pronounced local thinning due to direct contact with the forming tool, whereas the lower aluminum layer experiences moderated deformation owing to stress attenuation provided by the intermediate polyethylene core. The polymer layer plays a critical role in redistributing stresses and facilitating more uniform strain accommodation, thereby enhancing the overall formability of the laminate compared to single-layer aluminum sheets. The influence of key process parameters was systematically evaluated. Increases in feed rate and vertical step-down intensified localized strains and promoted higher thickness reduction, whereas higher spindle speeds improved material flow and mitigated excessive thinning. These findings underscore the importance of carefully selecting and optimizing TPIF parameters to achieve uniform thickness distribution and high-quality formed components. Overall, the Al–PE–Al sheet configuration exhibited superior formability compared to monolithic Aluminum sheets, suggesting that such hybrid laminates can be effectively employed to form components with complex geometries. The results provide valuable insights into the underlying deformation mechanisms of multilayer sheets under incremental forming and offer practical guidance for the design, optimization, and industrial application of these structures in lightweight and high-performance engineering components

Authors' contributions

M. Farhadi: Conceptualization**,** Material preparation, Data collection, Data analysis, Design, Writing original draft

B. Soltani: Conceptualization**,** Material preparation, Data collection, Data analysis, Design, Writing - review & editing

M. Honarpisheh: Conceptualization**,** Material preparation, Data collection, Data analysis, Design, Writing - review & editing

Conflict of interest

The authors have no competing interests to declare relevant to the content of this article.

Funding

The authors declare that no funds, grants, or other support were received during the preparation of this manuscript.

5. References

[1] Trzepieciński, T., Najm, S. M., Pepelnjak, T., Bensaid, K., & Szpunar, M. (2021). New advances and future possibilities in forming technology of hybrid metal–polymer composites used in aerospace applications. *Journal of Composites Science*, *5*(8), 217. https://doi.org/10.3390/jcs5080217

[2] Marques, A. E., Prates, P. A., Pereira, A. F. G., Sakharova, N. A., Oliveira, M. C., & Fernandes, J. V. (2020). Numerical study on the forming behaviour of multilayer sheets. *Metals*, *10*(6), 716. https://doi.org/10.3390/met10060716

[3] Maqbool, F., Maaß, F., Bühl, J., Hahn, M., Hajavifard, R., Walther, F., & Tekkaya, A. E. (2021). Targeted residual stress generation in single and two point incremental sheet forming (ISF). *Archive of Applied*

Mechanics, *91*, 3465–3487. https://doi.org/10.1007/s00419-021-01935-z

[4] Murugesan, M., Yu, J. H., Jung, K. S., Cho, S. M., Bhandari, K. S., & Lee, C. W. (2022). Optimization of forming parameters in incremental sheet forming of AA3003-H18 sheets using Taguchi method. *Materials*, *15*(4), 1458. https://doi.org/10.3390/ma15041458

[5] Gao, K., Zhang, X., Liu, B., He, J., Feng, J., Ji, P., Fang, W., & Yin, F. (2020). The deformation characteristics, fracture behavior and strengthening toughening mechanisms of laminated metal composites: A review. *Metals*, *10*(1), 4. https://doi.org/10.3390/met10010004

[6] T Majagi, S. D., Chandramohan, G., & Senthil Kumar, M. (2015). Effect of incremental forming process parameters on aluminum alloy using experimental studies. *Advanced Materials Research, 1119*, 633–639. https://doi.org/10.4028/www.scientific.net/amr.1119.633

[7] Popp, G. P., Racz, S. G., Breaz, R. E., Oleksik, V. Ș., Popp, M. O., Morar, D. E., Chicea, A. L., & Popp, I. O. (2024). State of the art in incremental forming: Process variants, tooling, industrial applications for complex part manufacturing and sustainability of the process. *Materials*, *17*(23), 5811. https://doi.org/10.3390/ma17235811

[8] Szpunar, M., Ostrowski, R., Trzepieciński, T., & Kaščák, Ľ. (2021). Central composite design optimisation in single point incremental forming of truncated cones from commercially pure titanium grade 2 sheet metals. *Materials*, *14*(13), 3634. https://doi.org/10.3390/ma14133634

[9] Ghasemi, H., & Soltani, B. (2014). Experimental investigation on the effective parameters on forming force, dimensional accuracy and thickness distribution in single point incremental forming. *Modares Mechanical Engineering*, *14*(1), 89–96. https://dor.isc.ac/dor/20.1001.1.10275940.1393.14.1.17.6

[10] Honarpisheh, M., Ebrahimi, M. R., & Mansouri, H. (2019). Investigation of springback angle in single point incremental forming process on explosive welded Cu/St/Cu multilayer. *Journal of Modern Processes in Manufacturing and Production*, *8*(3), 13–26. https://journals.iau.ir/article_664286.html

[11] Rezaei, H., & Honarpisheh, M. (2022). Experimental and numerical investigation of forming limit diagram of CP-Ti/St12 bimetal in incremental forming process. *Strength of Materials*, *54*(4), 681–694. https://doi.org/10.1007/s11223-022-00446-8

[12] Deilami Azodi, H., Rezaei, S., Beygi, A. Z., & Badparva, H. (2022). Investigation of parameters influencing forming force and thickness distribution in single point incremental forming of AA3105-St12 two-layer sheet. *Iranian Journal of Materials Forming*, *9*(2), 46–57. https://doi.org/10.22099/ijmf.2022.42993.1215

[13] Deilami Azodi, H., Rezaee, S., Badparva, B., & Zeinolabedin Beygi, A. (2022). Optimizing AA3105-St12 two-layer sheet in incremental sheet forming process using neural network and multi-objective genetic algorithm. *Modares Mechanical Engineering*, *22*(2), 121–132. SID. https://dor.isc.ac/dor/20.1001.1.10275940.1400.22.2.4.7

[14] Esmailian, M., Honarpisheh, M., & Gheysarian, A. (2023). Investigation of fracture depth of metal-polymer three layer sheet in single-point incremental forming process. *Iranian Journal of Materials Forming*, *10*(1), 39–52. https://doi.org/10.22099/ijmf.2023.46874.1249

[15] Tayebi, P., & Hashemi, R. (2024). Study of single point incremental forming limits of Al1050/Mg-AZ31B two-layer sheets fabricated by roll bonding technique: Finite element simulation and experiment. *Journal of Materials Research and Technology*, *29*, 149–169. https://doi.org/10.1016/j.jmrt.2024.01.085

[16] Tayebi, P., Nasirin, A. R., Akbari, H., & Hashemi, R. (2024). Experimental and numerical investigation of forming limit diagrams during single-point incremental forming for Al/Cu bimetallic sheets. *Metals*, *14*(2), 214. https://doi.org/10.3390/met14020214

[17] Li, X., Pan, J., Liu, L., Huang, Z., & Wang, Q. (2016). Effect of some process parameters on geometric errors in two point incremental forming for Al-Cu-Mg aluminum alloy. *Journal of Physics: Conference Series*, 734, 032078. https://doi.org/10.1088/1742-6596/734/3/032078

[18] Ou, L., An, Z., Gao, Z., Zhou, S., & Men, Z. (2020). Effects of Process Parameters on the Thickness Uniformity in two-point incremental forming (TPIF) with a positive die for an irregular stepped part. *Materials*, *13*(11), 2634. https://doi.org/10.3390/ma13112634

[19] Visagan, A., & Ganesh, P. (2022). Parametric optimization of two-point incremental forming using GRA and TOPSIS. *International Journal of Simulation Modelling*, *21*(4), 615–626. https://doi.org/10.2507/IJSIMM21-4-622

[20] Singal, A. H., Farhood, N. H., Al-Qassar, A. A. (2023). Experimental inspection of residual stresses induced in parts produced by two-point incremental forming (TPIF) process. *Journal of Engineering Science and Technology, 18*(1), 347–356. https://doi.org/10.3390/jeset1841

[21] Thokale, M., Gupta, R., & Sharma, V. (2024). Enhancing sheet metal forming through ultrasonic-assisted incremental techniques: A comparative analysis of SPIF

and TPIF. *SGVU International Journal of Convergence of Technology and Management*, *10*(2), 51–58.

[22] Harhash, M., & Palkowski, H. (2021). Incremental sheet forming of steel/polymer/steel sandwich composites. *Journal of Materials Research and Technology*, *13*, 417–430. https://doi.org/10.1016/j.jmrt.2021.04.088

[23] Trzepieciński, T., Najm, S. M., Pepelnjak, T., Bensaid, K., & Szpunar, M. (2022). Incremental sheet forming of metal-based composites used in aviation and automotive applications. *Journal of Composites Science*, *6*(10), 295. https://doi.org/10.3390/jcs6100295

[24] Zhao, X., & Ou, H. (2023). A new flexible multi-point incremental sheet forming process with multi-layer sheets. *Journal of Materials Processing Technology*, *322*, 118214. https://doi.org/10.1016/j.jmatprotec.2023.118214

[25] Zhao, X., & Ou, H. (2024). A new hybrid stretch forming and double-layer two-point incremental sheet forming process. *Journal of Materials Research and Technology*, *30*, 3485–3509. https://doi.org/10.1016/j.jmrt.2024.04.093

[26] Önal, Ü., Seçgin, Ö., Özsert, İ. et al. (2024). A new approach to multi-stage incremental forming method. *Arabian Journal for Science and Engineering*, *49*, 15325–15334. https://doi.org/10.1007/s13369-024-08970-2

[27] Maaß, F., Hahn, M., & Tekkaya, A. E. (2021). Adjusting residual stresses by flexible stress superposition in incremental sheet metal forming. *Archive of Applied Mechanics*, *91*, 3489–3499. https://doi.org/10.1007/s00419-021-01929-x

[28] Cen, H. T., Chi, L. X., & Li, H. (2009). An experimental study on composites machining using abrasive water jet technology. *Key Engineering Materials, 407–408*, 582–585. https://doi.org/10.4028/www.scientific.net/KEM.407-408.582